

substantially more susceptible to (and less able to clear) an ascending infection in the FRT than WT mice. Because NK cells have a protective role against this infection (16), we measured their levels at 3 days pi. Notably, both the percentage and total numbers of these cells were decreased in the uteri of *Ifn-ε*<sup>-/-</sup> mice (fig. S6, A and B). Importantly, there were no changes in *Ifn-ε* RNA expression at the early or late stages of the infection (fig. S6C), consistent with our in vitro data showing that *Ifn-ε* is not regulated by PRR pathways. Furthermore, production of *Ifn-β* and IRGs was higher than the levels in WT mice (fig. S7, A to D), indicating that the protective effects of *Ifn-ε* were not solely due to priming for the production of other type I IFNs. To demonstrate that *Ifn-ε* could directly mediate protection against infection, we observed a dose-dependent reduction in bacteria (Fig. 4E), demonstrating that reconstitution of (progesterone) lowered *Ifn-ε* levels protected against this bacterial infection.

The distinct properties of IFN-ε, compared with other type I IFNs (table S2), make IFN-ε the only one that protects against *Chlamydia*, whereas the others exacerbate disease (17–20). All type I IFNs protect against HSV-2 infection (21, 22), with IFN-ε likely contributing because its constitutive expression by epithelial cells offers immediate efficacy at the site of first contact of mucosal pathogens. Interestingly, the increased susceptibility to FRT infections of women on progestagen-containing contraception (23, 24) may be explained by the lowering of *Ifn-ε* levels (fig. S8A) during progestin pretreatment that is required for all FRT infection models (25, 26). The local effect of

IFN-ε is supported by our observation that IFN-ε makes no difference in a systemic model (fig. S8, B to D). Consistent with the importance of IFN-ε in FRT immunity, IFN-ε is evolutionarily conserved in eutherian mammals, particularly in residues predicted to contact the two receptor components (fig. S9) (27). Because STIs are major global health and socioeconomic problems, the distinctive regulatory and protective properties of IFN-ε may facilitate the development of new strategies for preventing and treating STIs and, perhaps, other diseases.

#### References and Notes

- S. Hervas-Stubbs et al., *Clin. Cancer Res.* **17**, 2619 (2011).
- A. Isaacs, J. Lindenmann, *Proc. R. Soc. London Ser. B Biol. Sci.* **147**, 258 (1957).
- M. P. Hardy, C. M. Owczarek, L. S. Jermiin, M. Ejdeback, P. J. Hertzog, *Genomics* **84**, 331 (2004).
- K. Honda, A. Takaoka, T. Taniguchi, *Immunity* **25**, 349 (2006).
- M. Sato et al., *Immunity* **13**, 539 (2000).
- N. A. de Weerd, S. A. Samarajiwa, P. J. Hertzog, *J. Biol. Chem.* **282**, 20053 (2007).
- L. Alexopoulou, A. C. Holt, R. Medzhitov, R. A. Flavell, *Nature* **413**, 732 (2001).
- S. E. Doyle et al., *J. Immunol.* **170**, 3565 (2003).
- V. Hornung, E. Latz, *Nat. Rev. Immunol.* **10**, 123 (2010).
- M. V. Patel, M. Ghosh, J. V. Fahey, C. R. Wira, *PLoS ONE* **7**, e35654 (2012).
- L. A. Salamonsen, in *The Endometrium*, J. D. Aplin, A. T. Fazleabas, S. R. Glasser, L. C. Giudice, Eds. (Informa Healthcare, London, ed. 2, 2008), pp. 25–45.
- M. Thapa, D. J. Carr, *J. Virol.* **83**, 9486 (2009).
- K. W. Beagley, W. M. Huston, P. M. Hansbro, P. Timms, *Crit. Rev. Immunol.* **29**, 275 (2009).
- World Health Organization (WHO), *Global Prevalence and Incidence of Selected Curable Sexually Transmitted Infections Overview and Estimates* (WHO, Geneva, 2001).
- K. L. Asquith et al., *PLoS Pathog.* **7**, e1001339 (2011).
- C. T. Tseng, R. G. Rank, *Infect. Immun.* **66**, 5867 (1998).

- A. Devitt, P. A. Lund, A. G. Morris, J. H. Pearce, *Infect. Immun.* **64**, 3951 (1996).
- S. P. Lad, E. Y. Fukuda, J. Li, L. M. de la Maza, E. Li, *J. Immunol.* **174**, 7186 (2005).
- U. M. Nagarajan, D. M. Ojcius, L. Stahl, R. G. Rank, T. Darville, *J. Immunol.* **175**, 450 (2005).
- U. M. Nagarajan et al., *Infect. Immun.* **76**, 4642 (2008).
- B. A. Austin, C. M. James, P. Härle, D. J. Carr, *Biol. Proced. Online* **8**, 55 (2006).
- C. D. Conrady, W. P. Halford, D. J. Carr, *J. Virol.* **85**, 1625 (2011).
- J. M. Baeten et al., *Am. J. Obstet. Gynecol.* **185**, 380 (2001).
- C. C. Wang, J. K. Kreiss, M. Reilly, *J. Acquir. Immune Defic. Syndr.* **21**, 51 (1999).
- R. P. Morrison, H. D. Caldwell, *Infect. Immun.* **70**, 2741 (2002).
- M. B. Parr et al., *Lab. Invest.* **70**, 369 (1994).
- C. Thomas et al., *Cell* **146**, 621 (2011).

**Acknowledgments:** We thank A. Mansell, R. Ferrero, and L. Salamonsen for their contributions; N. Bourke and S. Forster for helpful discussions and reading of the manuscript; K. Fitzgerald for reagents; and C. Berry for assistance with viral plaque assays. The data presented in this paper are tabulated in the main text and in the supplementary materials. This work was supported by funding from Australian National Health and Medical Research Council (P.J.H., N.E.M., P.M.H., J.R., C.E.G., and B.P.), the Australian Research Council (P.J.H., N.E.M., J.R.), the NIH via grant R01 AI053108 (D.J.C.), and the Victorian Government's Operational Infrastructure Support Program. P.J.H., N.E.M., K.Y.F., H.C., S.A.S., and N.D.W. hold International Patent Application number PCT/AU2011/000715, "Use of interferon epsilon in methods of diagnosis and treatment."

#### Supplementary Materials

[www.sciencemag.org/cgi/content/full/339/6123/1088/DC1](http://www.sciencemag.org/cgi/content/full/339/6123/1088/DC1)  
Materials and Methods  
Figs. S1 to S9  
Tables S1 and S2  
References (28–33)  
28 November 2012; accepted 8 January 2013  
10.1126/science.1233321

the rat (10, 13). Similarly, there is a 20- to 30-min delay between the end of the aura and the headache (14). Such time lags may be required for transduction of algic signals over glia limitans via inflammatory mediators. Intense depolarization and N-methyl-D-aspartate (NMDA) receptor overactivation opens neuronal Pannexin1 (Panx1) megachannels (15–17). These conditions are present during CSD and suggest that CSD, by activating Panx1 and downstream inflammasome formation, may trigger inflammation (17, 18). We therefore hypothesize that stress-induced Panx1 activation may cause headache by releasing pro-inflammatory mediators such as high-mobility group box 1 (HMGB1) from neurons, which initiates a parenchymal inflammatory response, leading to sustained release of inflammatory mediators from glia limitans and, hence, prolonged trigeminal stimulation.

Propidium iodide (PI) is a membrane-impermeable fluoroprobe used to monitor activity as it passes through megachannels such as

<sup>1</sup>Institute of Neurological Sciences and Psychiatry, Hacettepe University, Ankara 06100, Turkey. <sup>2</sup>Department of Neurology, Faculty of Medicine, Hacettepe University, Ankara 06100, Turkey. <sup>3</sup>Department of Psychiatry, Faculty of Medicine, Hacettepe University, Ankara 06100, Turkey.

\*To whom correspondence should be addressed. E-mail: tdalkara@hacettepe.edu.tr

## Spreading Depression Triggers Headache by Activating Neuronal Panx1 Channels

Hulya Karatas,<sup>1,2</sup> Sefik Evren Erdener,<sup>1,2</sup> Yasemin Gursoy-Ozdemir,<sup>1,2</sup> Sevda Lule,<sup>1</sup> Emine Eren-Koçak,<sup>1,3</sup> Zümrüt Duygu Sen,<sup>1,3</sup> Turgay Dalkara<sup>1,2\*</sup>

The initial phase in the development of a migraine is still poorly understood. Here, we describe a previously unknown signaling pathway between stressed neurons and trigeminal afferents during cortical spreading depression (CSD), the putative cause of migraine aura and headache. CSD caused neuronal Pannexin1 (Panx1) megachannel opening and caspase-1 activation followed by high-mobility group box 1 (HMGB1) release from neurons and nuclear factor κB activation in astrocytes. Suppression of this cascade abolished CSD-induced trigeminovascular activation, dural mast cell degranulation, and headache. CSD-induced neuronal megachannel opening may promote sustained activation of trigeminal afferents via parenchymal inflammatory cascades reaching glia limitans. This pathway may function to alarm an organism with headache when neurons are stressed.

There is agreement that activation of the trigeminocervical complex mediates migraine headache, whereas the brain event that initiates migraine is unclear (1–3). Cortical spreading depression (CSD) thought to cause the migraine aura may activate perivascular trigeminal nerves (4–10) by way of potassium, protons, nitric oxide (NO), arachidonic acid, and adenosine

5'-triphosphate released during CSD (3, 8, 11). However, sufficient concentrations of these mediators may not be sustained in the perivascular space for trigeminal sensitization and hours-lasting headache (10, 12) because of the glia limitans barrier and continuous cerebrospinal fluid (CSF) flow. Trigeminal meningeal nociceptors and central neurons also start firing ~14 and 25 min after CSD in

**Fig. 1.** CSD causes neuronal Panx1 channel opening, caspase-1 activation, and HMGB1 release. A single CSD triggered by pinprick to the intact mouse brain (**A**) caused PI influx (red fluorescence) to cortical (Cx) and dentate (DG) neurons, (**B**) identified with Hoechst-33258. PI was injected intracerebroventricularly 2 min before CSD. Non-specific labeling of the ventricular lining (VL) marked successful PI injection (low-magnification images were contrast/brightness-adjusted for better illustration). (**C**, **M**, and **N**) PI-influx was suppressed by Panx1 inhibitors carbenoxolone (CBX), probenecid (Pro), or  $^{10}\text{Panx}$ . (**D** to **F**) PI-labeled cells were NeuN-positive neurons. (**G** and **H**) PI-positive neurons exhibited cleaved caspase-1 immunoreactivity 5 min after CSD. (**I**) A robust HMGB1 and IL-1 $\beta$  release to CSF was detected after KCl-induced CSDs, unlike sham-operated mice. HMGB1-shRNA suppressed HMGB1 release to CSF. (**J** and **K**) Neuronal nuclei lost their HMGB1-immunopositivity 30 min after CSD, which (**L**) was prevented by CBX pre-treatment. Number of PI-positive neurons was maximum 5 min after CSD and disappeared in an hour in ipsi- and contralateral cortex (**M**) and DG (**N**) (error bars, SEM, 3 to 6 mice for each time points).

PI-labeling was inhibited when CSD generation was suppressed by means of epidural MK-801 application (10 mM adsorbed into a cotton ball) to the pinprick site [**(M)** and **(N)**]. Panx1 inhibitors abolished PI-labeling evaluated

5 min after CSD [**(M)** and **(N)**]. CBX did not modify CSD generation and propagation (CSDs recorded with 2 electrodes 1 mm apart are shown in inset). Scale bars, 20  $\mu\text{m}$ .

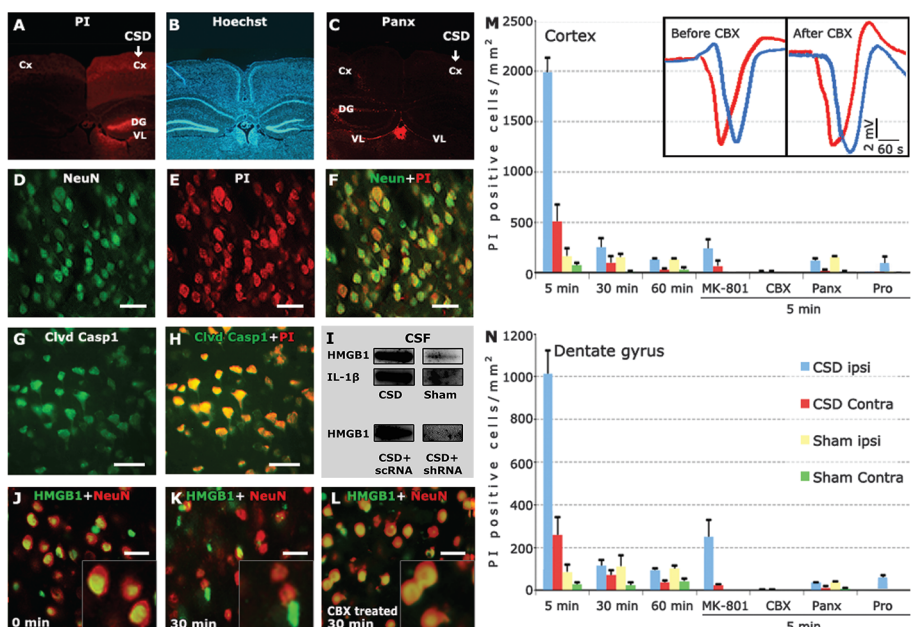
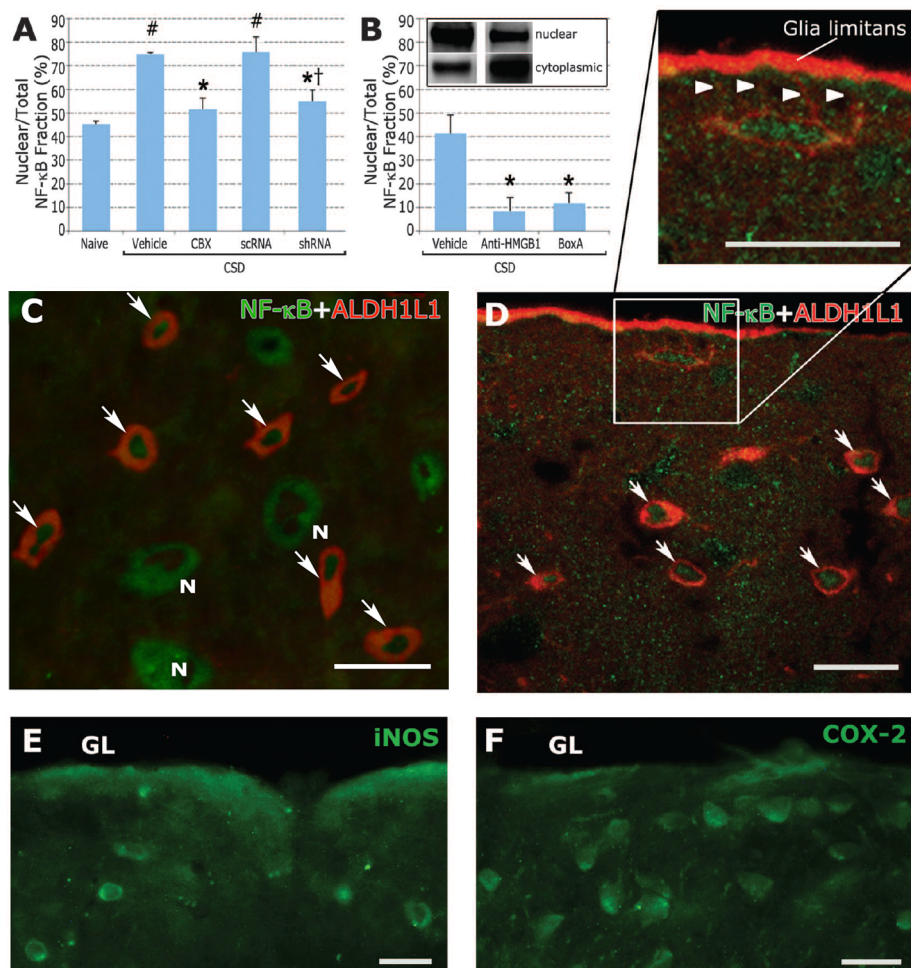


**Fig. 2.** CSD induces NF- $\kappa$ B translocation reversed by inhibition of Panx1 channels or HMGB1. (**A** and **B**) Western blotting of cytoplasmic and nuclear brain fractions shows that CSD induces translocation of NF- $\kappa$ B from cytoplasm to nucleus in cortex within 30 min. This is prevented by Panx1 channel inhibition (CBX), by silencing HMGB1 expression, BoxA, and antibody to HMGB1. Columns represent mean  $\pm$  SEM from 3 to 4 mice,  $P \leq 0.05$  compared with naive (#) and vehicle-treated (\*) groups.  $P = 0.08$  compared with the scrambled shRNA-treated group (†). Unlike groups in (A), BoxA and antibody to HMGB1 (B) were injected intracortically just before CSD without any prior injections to the brain (19); hence, they exhibited different NF- $\kappa$ B levels. (**C**) Thirty min after CSD, astrocytes identified with ALDH1L1 immunoreactivity (red) displayed nuclear NF- $\kappa$ B-immunoreactivity (green nuclei, arrows), unlike normal cytoplasmic NF- $\kappa$ B immunostaining seen in neurons (N). (**D**) NF- $\kappa$ B translocation was observed all over the cortex, including astrocytes forming (arrowheads in blown-up image) or abutting glia limitans (GL). (**E** and **F**) NF- $\kappa$ B translocation was followed by COX2 and iNOS induction in astrocytes and GL. Scale bars, 20  $\mu\text{m}$ .



Panx1 (15, 19). In mouse brain *in vivo*, single or multiple CSDs triggered by pinprick or KCl caused PI influx to cortical and dentate neurons ( $95 \pm 3\%$ , mean  $\pm$  SEM, of PI-labeled cells were NeuN-positive) (Fig. 1). PI uptake was inhibited by Panx1 channel blockers carbinoxolone (CBX) [400 ng intracerebroventricularly (icv)], probenecid (60  $\mu$ g icv),  $^{10}\text{Panx}$  (100  $\mu\text{M}$  intracortical), or Panx1-small interfering RNA (siRNA) (Fig. 1, M and N, and fig. S1) (19). Vehicle alone or nonsilencing siRNA had no effect. CBX and  $^{10}\text{Panx}$  did not affect CSD generation and propagation, suggesting that prevention of PI uptake was not caused by CSD suppression (Fig. 1). No PI uptake was observed in astrocytes (fig. S2A). PI labeling was maximal 5 min after CSD and disappeared in an hour, possibly because of active extrusion of PI from live cells *in vivo*. PI uptake was not caused by intracerebroventricular injection (19) because it could be inhibited when CSD generation was suppressed by epidural MK-801 application to the pinprick site. During CSD, cells did not take up FITC-dextran-70S, which is also membrane impermeable but too large to pass through megapores, indicating that PI influx was not due to osmotic rupture of the plasma membrane (additional control experiments are available in the supplementary text).

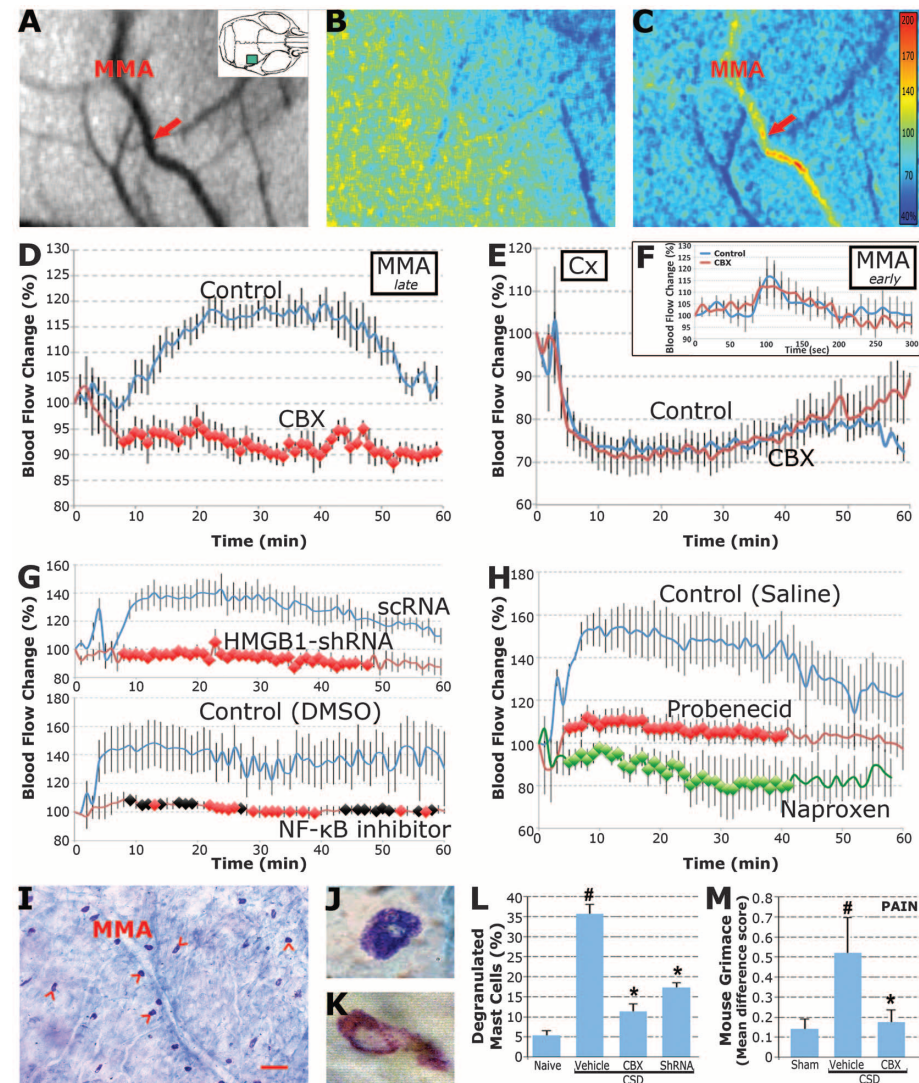
Caspase-1 was activated in  $99.2 \pm 0.2\%$  of PI-positive neurons 5 min after CSD (Fig. 1H). Caspase-1 activation initiates inflammation by releasing HMGB1 and interleukin-1 $\beta$  (IL-1 $\beta$ ) (17, 18, 20). Indeed, CSF collected from lateral ventricles of mice subjected to CSDs for 1 hour showed a 10-fold HMGB1 and 24-fold IL-1 $\beta$  increase in Western blots (Fig. 1I). HMGB1-short hairpin RNA (shRNA) suppressed HMGB1 release to CSF (19) (Fig. 1I and fig. S3). Double-staining of brain sections illustrated that  $88.0 \pm 0.1\%$  and  $52 \pm 4\%$  of neurons were HMGB1-positive 5 and 30 min after a single CSD, although all neuronal nuclei were HMGB1-positive without CSD (Fig. 1, J and K). CBX abolished cleaved caspase-1 immunoreactivity and HMGB1 translocation in addition to inhibiting PI-positivity (Fig. 1, L to N).

CSD also induced nuclear factor  $\kappa$ B (NF- $\kappa$ B) activation; most astrocytes ( $82 \pm 6\%$ ) exhibited

nuclear NF- $\kappa$ B translocation 30 min after CSD (Fig. 2). CBX inhibited NF- $\kappa$ B translocation, suggesting that the signal leading to NF- $\kappa$ B translocation was initiated by the opening of Panx1 channels and release of HMGB1 (Fig. 2A and figs. S2B and S4). Indeed, NF- $\kappa$ B translocation was also inhibited with neutralizing antibody to HMGB1; BoxA, a fragment of HMGB1 with antagonistic activity; or HMGB1-shRNA (Fig. 2 and fig. S2C) (19). Astrocytes forming glia limitans also showed nuclear NF- $\kappa$ B translocation followed by cyclooxygenase-2 (COX2) and inducible nitric oxide synthase (iNOS) induction after CSD, which can provide the sustained inflammatory mediator release to subarachnoid space (Fig. 2, C to F).

As reported in the rat (8), CSD induced an early, brief ( $21 \pm 1$  s) flow increase followed by a late (peak latency;  $21 \pm 2$  min) but sustained ( $51 \pm 3$  min) blood flow elevation in ipsilateral middle meningeal artery (MMA) in mice (Fig. 3). CSD-induced late MMA dilation, which is initiated by activation of the trigeminal nerves around pial vessels (8), was completely inhibited with CBX (Fig. 3D), suggesting that Panx1 channel opening

**Fig. 3.** Inhibition of Panx1 channels or inflammatory mediators suppresses trigeminovascular activation. (A) Speckle contrast images of the MMA and cortex were captured through thinned skull (inset, green rectangular area) before CSD. Color bar in (C) indicates the relative blood flow change to baseline. (B) The relative blood flow image obtained 2 min after pinprick-induced CSD shows the early cortical oligemia (blue) spreading from anterior to posterior. (C) Twenty-five min after CSD, there is selective flow increase in the MMA (red arrow), whereas the cortex is still hypoperfused. (D and E) The time course of blood flow changes in the ipsilateral MMA and cortex after CSD (vertical bars  $\pm$ SEM). Late blood flow elevation in MMA was inhibited with CBX. CBX did not affect cortical blood flow (E) or early and brief MMA flow increase, which (F) can be correctly displayed only with an expanded time scale (19). (G and H) CSD-induced late MMA flow increase was also suppressed by HMGB1-shRNA, NF- $\kappa$ B inhibitor, probenecid, and naproxen. Diamonds indicate significant difference ( $P < 0.05$ ) as compared with corresponding controls (black diamonds;  $P < 0.07$ ). CBX treatment and HMGB1 silencing also inhibited CSD-induced dural MAST cell degranulation, another manifestation of the trigeminovascular activation. (I) The dura with mast cells concentrated along the course of MMA. Scale bar, 100  $\mu\text{m}$ . (J and K) Examples of a resting and a degranulated mast cell, respectively. (L) The percentage of mast cells degranulated 30 min after CSD in ipsilateral dura.  $P < 0.05$  compared with naive (#) and vehicle-treated (\*) groups. (M) CSD-induced pain was assessed by means of mouse grimace scale. Mean difference scores from the baseline show that repeated CSDs induced by a KCl pellet over the dura caused pain-related mimics, which was significantly suppressed by CBX pretreatment. In the sham group, saline was applied over the dura.



and downstream inflammatory cascade play a role in trigeminal activation. The effect of CBX was not due to a direct vascular action or blockade of gap junctions because CSD-induced CBF changes, early MMA dilation, and  $\text{Ca}^{2+}$  rise in astrocytic syncytium were not altered by CBX (Fig. 3, E and F, and fig. S5) (19). Interrupting this signaling cascade with another Panx1 inhibitor, probenecid or HMGB1-shRNA, or NF- $\kappa$ B activation inhibitor 4-methyl-N1-(3-phenylpropyl) benzene-1,2-diamine suppressed the late MMA dilation (Fig. 3, G and H). Naproxen (40 mg/kg intraperitoneally), a prostaglandin synthase inhibitor, also suppressed the MMA response. Moreover, CSD-induced dural mast cell degranulation, another manifestation of the trigeminal activation (21, 22), was significantly reduced by CBX and HMGB1-shRNA (Fig. 3, I to L). Last, we assessed the headache-like behavior induced by repeated CSDs (which also induced PI influx and nuclear NF- $\kappa$ B translocation) (19) with a method based on scoring facial grimace (23). Placement of a KCl-pellet over dura in freely moving mice caused pain-related mimics unlike saline-applied, sham-operated mice. CSD-induced pain was reversed by means of CBX treatment (Fig. 3M).

These data show that CSD opens neuronal Panx1 channels as reported during *in vitro* ischemia, NMDA over-activation, and aberrant bursting (17). Activation of Panx1 by cellular stressors such as excess potassium or glutamate stimulates the inflammasome complex, subsequent caspase-1 activation, and IL-1 $\beta$  production (17, 18), suggesting that Panx1 megachannels may play a role as a reporter linking neuronal stress to inflammatory response. Similarly, CSD induced caspase-1 activation and HMGB1 release from neurons whose Panx1 channels were activated.

HMGB1 is a member of the alarmin family, which mediates the communication between injured and surrounding cells (24). HMGB1 is passively released from necrotic cells and actively secreted by cells under distress (25, 26). HMGB1 behaves like a cytokine and promotes inflammation when released (27, 28). Therefore, HMGB1 and IL-1 $\beta$  released during CSD may take part in initiation of the inflammatory response. Subsequent NF- $\kappa$ B activation in astrocytes may induce formation of cytokines, prostanoids, and inducible NO synthase-derived NO (as suggested by inhibition of MMA response by naproxen and CSD-induced COX2 and iNOS expression in glia limitans), which may be released to the subarachnoid space via glia limitans and, hence, stimulate trigeminal nerve endings around pial vessels (fig. S6). By promoting sustained headache, HMGB1 may thus serve to alarm the organism that the brain parenchyma has been stressed by CSD or CSD-like events. HMGB1 is most likely not the only mediator playing this role; other cytokines as well as cells (such as microglia) may also take part along the course of inflammatory response (29, 30). In contrast to mediators such as potassium and protons that are transiently released during CSD, activation of the parenchymal in-

flammatory pathways may provide the sustained stimulus required for sensitization of trigeminal nerve endings and lasting pain as suggested by suppression of long-lasting MMA vasodilatation, mast cell degranulation, and importantly, headache-like behavior by interrupting the inflammatory cascade at one of the steps (11).

We propose a previously unknown link between a noxious intrinsic brain event and activation of the trigeminal pain fibers, involving the opening of Panx1 megachannels on stressed neurons, subsequent activation of the inflammatory pathways, and transduction of this signal to the trigeminal nerves around pial vessels (fig. S6).

#### References and Notes

- M. A. Moskowitz, *Headache* **48**, 688 (2008).
- P. J. Goadsby, *Trends Mol. Med.* **13**, 39 (2007).
- J. Olesen, R. Burstein, M. Ashina, P. Tfelt-Hansen, *Lancet Neurol.* **8**, 679 (2009).
- M. A. Moskowitz, *Ann. Neurol.* **16**, 157 (1984).
- M. A. Moskowitz, K. Nozaki, R. P. Kraig, *J. Neurosci.* **13**, 1167 (1993).
- M. Lauritzen, *Brain* **117**, 199 (1994).
- T. Dalkara, N. T. Zervas, M. A. Moskowitz, *Neurol. Sci.* **27**, (Suppl 2), S86 (2006).
- H. Bolay *et al.*, *Nat. Med.* **8**, 136 (2002).
- N. Hadjikhani *et al.*, *Proc. Natl. Acad. Sci. U.S.A.* **98**, 4687 (2001).
- X. Zhang *et al.*, *J. Neurosci.* **30**, 8807 (2010).
- D. Levy, *Curr. Pain Headache Rep.* **16**, 270 (2012).
- A. M. Strassman, S. A. Raymond, R. Burstein, *Nature* **384**, 560 (1996).
- X. Zhang *et al.*, *Ann. Neurol.* **69**, 855 (2011).
- J. Olesen *et al.*, *Ann. Neurol.* **28**, 791 (1990).
- R. J. Thompson, N. Zhou, B. A. MacVicar, *Science* **312**, 924 (2006).
- R. J. Thompson *et al.*, *Science* **322**, 1555 (2008).
- B. A. MacVicar, R. J. Thompson, *Trends Neurosci.* **33**, 93 (2010).
- W. R. Silverman *et al.*, *J. Biol. Chem.* **284**, 18143 (2009).
- Materials and methods are available as supplementary materials on *Science Online*.
- M. Lamkanfi *et al.*, *J. Immunol.* **185**, 4385 (2010).
- S. Markowitz, K. Saito, M. G. Buzzi, M. A. Moskowitz, *Brain Res.* **477**, 157 (1989).
- D. Levy, R. Burstein, V. Kainz, M. Jakubowski, A. M. Strassman, *Pain* **130**, 166 (2007).
- D. J. Langford *et al.*, *Nat. Methods* **7**, 447 (2010).
- D. S. Pisetsky, H. Erlandsson-Harris, U. Andersson, *Arthritis Res. Ther.* **10**, 209 (2008).
- P. Scalfidi, T. Misteli, M. E. Bianchi, *Nature* **418**, 191 (2002).
- S. Müller, L. Ronfani, M. E. Bianchi, *J. Intern. Med.* **255**, 332 (2004).
- G. Faraco *et al.*, *J. Neurochem.* **103**, 590 (2007).
- M. Pedrazzi *et al.*, *J. Immunol.* **179**, 8525 (2007).
- P. E. Kunkler, R. E. Hulse, R. P. Kraig, *J. Cereb. Blood Flow Metab.* **24**, 829 (2004).
- S. Jander, M. Schroeter, O. Peters, O. W. Witte, G. Stoll, *J. Cereb. Blood Flow Metab.* **21**, 218 (2001).

**Acknowledgments:** We are grateful to M. A. Moskowitz for helpful discussions, K. Kilic and E. Lule for their expert help with the figures, and to A. Can for his help with confocal microscopy. This work was supported by the Turkish Academy of Sciences (T.D.), Hacettepe University Research Fund 08-D07-101-011 (Y.G.-O.), and the Brain Research Association (H.K.).

#### Supplementary Materials

[www.sciencemag.org/cgi/content/full/339/6123/1092/DC1](http://www.sciencemag.org/cgi/content/full/339/6123/1092/DC1)  
Materials and Methods

Supplementary Text

Figs. S1 to S5

Table S1

References (31–42)

23 October 2012; accepted 30 January 2013  
10.1126/science.1231897

## Stress in Puberty Unmasks Latent Neuropathological Consequences of Prenatal Immune Activation in Mice

Sandra Giovanoli,<sup>1,2</sup> Harald Engler,<sup>3</sup> Andrea Engler,<sup>3</sup> Juliet Richetto,<sup>4,5</sup> Mareike Voigt,<sup>6,7</sup> Roman Willi,<sup>8</sup> Christine Winter,<sup>7</sup> Marco A. Riva,<sup>4,5</sup> Preben B. Mortensen,<sup>9,10</sup> Joram Feldon,<sup>2</sup> Manfred Schedlowski,<sup>3</sup> Urs Meyer<sup>1,2,\*</sup>

Prenatal infection and exposure to traumatizing experiences during peripuberty have each been associated with increased risk for neuropsychiatric disorders. Evidence is lacking for the cumulative impact of such prenatal and postnatal environmental challenges on brain functions and vulnerability to psychiatric disease. Here, we show in a translational mouse model that combined exposure to prenatal immune challenge and peripubertal stress induces synergistic pathological effects on adult behavioral functions and neurochemistry. We further demonstrate that the prenatal insult markedly increases the vulnerability of the pubescent offspring to brain immune changes in response to stress. Our findings reveal interactions between two adverse environmental factors that have individually been associated with neuropsychiatric disease and support theories that mental illnesses with delayed onsets involve multiple environmental hits.

**P**renatal maternal infection and postnatal exposure to psychological trauma are two environmental risk factors for developmental psychiatric disorders, including autism, schizophrenia, and bipolar disorder (1–4). In spite of their relatively frequent occurrence (5–7), both factors seem to have rather modest effect sizes

in large populations (4, 8, 9). For example, the global incidence of schizophrenia after influenza pandemics only increases marginally (relative risk ratios of 1 to 2.5) even though 20 to 50% of the general population is typically infected during influenza pandemics (9, 10). It has therefore been proposed that developmental stressors, such as

## Spreading Depression Triggers Headache by Activating Neuronal Panx1 Channels

Hulya Karatas, Sefik Evren Erdener, Yasemin Gursoy-Ozdemir, Sevda Lule, Emine Eren-Koçak, Zümrüt Duygu Sen, and Turgay Dalkara

Science, 339 (6123), • DOI: 10.1126/science.1231897

### How Migraine Develops

Migraine is a common medical disorder. Unfortunately, how and why migraine headache is initiated is unclear. Karatas *et al.* (p. 1092) now describe a signaling pathway between stressed neurons and meningeal trigeminal afferents, which may explain how migraine headaches can be generated.

### View the article online

<https://www.science.org/doi/10.1126/science.1231897>

### Permissions

<https://www.science.org/help/reprints-and-permissions>